The influence of PM$_{2.5}$ on lung injury and cytokines in mice

JIE YANG[1], YI CHEN[2], ZHI YU[3], HUI DING[3] and ZHONGFU MA[2]

[1]Department of Dermatology, Guangdong Academy of Medical Sciences (Guangdong General Hospital);
[2]Department of General Internal Medicine, The First Affiliated Hospital of Sun Yat-sen University, Guangzhou,
Guangdong 510080; [3]Research Center of Intelligent Transportation System, School of Engineering,
Sun Yat-sen University, Guangzhou, Guangdong 510275, P.R. China

Abstract. Exposure to particulate matter ≤2.5 μm in diameter (PM$_{2.5}$) profoundly affects human health. However, the role of PM$_{2.5}$ on lung injury and cytokine levels in mice is currently unknown. The aim was to examine the effect of PM$_{2.5}$ pollution on lung injury in mice fed at an underground parking lot. A total of 20 female Kunming mice were randomly divided into control and polluted groups, with 10 rats in each group. The control group was kept in the laboratory, while the pollution group was fed in an underground parking lot. The concentrations of pollutants were measured using ambient air quality monitoring instruments. After 3 months of treatment, the lungs were collected and examined using electron microscopy, and the morphological structures were assessed using hematoxylin and eosin staining. The polarization of macrophages was evaluated by immunofluorescence. The concentration of interleukin (IL)-4, tumor necrosis factor (TNF)-α and transforming growth factor (TGF)-β1 in peripheral sera were assessed by ELISA. The mRNA and protein levels of IL-4, TNF-α, and TGF-β1 in lung tissues were assessed by reverse transcription-quantitative polymerase chain reaction and western blot analyses, respectively. In the polluted group, the levels of CO, NO$_x$ and PM$_{2.5}$ were significantly higher compared with the control group. Compared with the controls, intracellular edema, an increased number of microvilli and lamellar bodies, smaller lamellar bodies in type II alveolar epithelial cells, and abundant particles induced by PM$_{2.5}$ in macrophages were observed in the polluted group. The lung ultrastructure changed in the polluted group, revealing exhaust-induced lung injury: The tissues were damaged, and the number of inflammatory cells, neutrophils, polylymphocytes and eosinophils increased in the polluted group compared with the control group. The authors also observed that the number of M1 and M2 macrophages markedly increased after the exhaust treatment. The levels of IL-4, TNF-α and TGF-β1 in the sera and tissues were significantly increased in the polluted group. PM$_{2.5}$ pollutants in underground garages can lead to lung injury and have a significant impact on the level of inflammatory cytokines in mice. Therefore, the authors suggest that PM$_{2.5}$ can activate the inflammatory reaction and induce immune dysfunction, leading to ultrastructural damage.

Introduction

With the rapid increase in the number of motor vehicles, the air quality in cities is increasingly deteriorating (1). Fine particles [particulate matter with an aerodynamic diameter smaller than 2.5 μm (PM$_{2.5}$)] cause ozone pollution, which leads to secondary pollution by oxidized pollutants under specific meteorological conditions, which in turn directly influence the health of most inhabitants in a polluted environment (1,2). Due to the characteristics of road traffic distribution, a considerable part of the population is under long-term exposure to serious PM$_{2.5}$ pollution in such a polluted environment (3,4). Thus, the health risks of PM$_{2.5}$ pollution cannot be ignored (1,2). Therefore, research on the effects of exhaust pollution on the human body, as well as the development of effective protection technologies, is necessary.

Diesel exhaust is not a single component, but a mixture of hundreds of gaseous and solid pollutants (5-7). Among them, the fine solid particles are mainly responsible for chronic lung injury. Pollutants in the range from PM$_{2.5}$ to PM$_{10}$ have been demonstrated to induce respiratory burst in RAW264.7 cells and could induce chronic lung injury (8-10). Previous studies showed that numerous acute toxicological experiments using single components of diesel exhaust confirmed that a variety of exhaust components can lead to an increased production of oxygen free radicals, thus directly damaging lung cells, and influencing digestive function, growth and development by negatively affecting Ca^{2+} balance (11,12). *In vivo* studies have revealed that the expression of transforming growth factor (TGF)-β1 is positively correlated with the duration of exposure to and the amount of atmospheric particulate matter, such as PM$_{2.5}$, in the environment (13-17). It was also demonstrated that the serum levels of interleukin (IL)-4 and tumor necrosis factor (TNF)-α are positively correlated with the duration of

Correspondence to: Dr Zhongfu Ma, Department of General Internal Medicine, The First Affiliated Hospital of Sun Yat-sen University, 58 2nd Zhongshan Road, Guangzhou, Guangdong 510080, P.R. China
E-mail: 1362670488@qq.com; mzf7773@126.com

exposure to air pollution, and that IL-4 levels were correlated with gaseous pollutants, such as NO_x, while TNF-α levels were correlated with particulate matter, such as $PM_{2.5}$ (18,19). In a study of the morphological changes in chronic lung injury of rats caused by gasoline exhaust pollution, inflammatory reactions were observed in the first 2 weeks, followed by lung fibroblast hyperplasia after 4 weeks (20). The hyperplasia of fibroblasts was increasingly evident with time and has been associated with chronic inflammatory reaction (21-23). However, the detailed changes in macrophage morphology and the macrophage M1-M2 balance remain unclear.

The air quality in the Central Laboratory of the First Affiliated Hospital of Sun Yat-sen University used by our group meets the requirements of GB3095-2012 standard class II of China (24), while the pollution levels exceed the national standard in underground parking lots. In the current study, the authors evaluated the levels of three representative indicators of pollution: CO, NO_x and $PM_{2.5}$, in an underground parking lot and the laboratory. After living in the environment for 3 months, the ultrastructure in the lungs of mice was examined by electron microscopy, and morphological structures were detected by hematoxylin and eosin (H&E) staining. To study the changes in the macrophage M1-M2 balance, double fluorescence staining of adhesion G protein-coupled receptor E1 (F4/80) with human leukocyte antigen (HLA)-DR or cluster of differentiation (CD)163 was further performed in lung tissue sections.

Materials and methods

Animals. A total of 20 female Kunming mice, 8-10 weeks old, weighing 22-25 g, were provided and approved by the Experimental Animal Ethics Committee Center of The First Affiliated Hospital of Sun Yat-sen University (Guangzhou, China; animal certificate no. 4408500931). The mice were randomly divided into two groups: Control and polluted (10 mice per group).

Feeding location and exposure to pollution. The mice were housed as previously described (25). In brief, the mice were housed at the Central Laboratory of the First Affiliated Hospital of Sun Yat-sen University in a controlled environment (food and water available *ad libitum*, 21±1˚C, 60% humidity and 12-h light/dark cycle). The mice in the polluted group were fed at the Second underground passage in a parking lot at the southeast corner of the First Affiliated Hospital of Sun Yat-sen University: At this location, there was a high flux of cars, and it was far from the exit and exhaust air outlets, therefore it had a relatively high level of pollution.

As described previously (26), $PM_{2.5}$ samples were collected using a Thermo Anderson G-2.5 air sampler (FH62C14, Model GV 2630 Series; Thermo Fisher Scientific, Inc., Waltham, MA, USA) that was installed in glass fiber filters. Firstly, the filters were heated at 200˚C for 24 h prior to sampling. Then, the filters were cut into small pieces, immersed in 0.9% saline and sonicated. The $PM_{2.5}$ suspension was vacuum-freeze dried and diluted with sterilized 0.9% physiological saline.

As described previously (27), the mice in the polluted group were treated with $PM_{2.5}$ at 20 mg/kg body weight for 3 days (once every other day). The mice in the control group were fed in the animal laboratory in The First Affiliated Hospital

of Sun Yat-sen University. During the feeding period, all mice were free to eat and drink. The mice were treated and fed as described for 3 months. Live mice were injected with inhalational anesthetics, and then were sacrificed humanely using carbon dioxide asphyxiation. The mice were necropsied soon following the completion of the exposure protocol. During the study the body weight was assessed every 3 days.

Determination of the concentration of pollutants. Measurements of the concentration of pollutants in the cages in the underground garage and in the laboratory were performed using three ambient air quality monitoring instruments. The concentration of NO_x was measured at the designated time-points using a 42C chemiluminescence NO-NO_2-NO_x analyzer (Thermo Environmental Instruments; Thermo Fisher Scientific, Inc.). For the determination of $PM_{2.5}$ concentration (28), a β-ray particle monitoring instrument (model FH62C14; Thermo Fisher Scientific, Inc.) was used to measure the attenuation of β-rays through the particles suspended in the air. CO concentration was determined using a gas correlation infrared CO analyzer (model 48C; Thermo Environmental Instruments; Thermo Fisher Scientific, Inc.). The concentrations of pollutants at the two feeding locations were measured 12 times a day.

Electron microscopy examination. Lung tissues samples were examined using electron microscopy as previously described (29,30). In brief, the mice were sacrificed, and the lung tissues were removed. Lung tissue samples were fixed with 2.5% glutaraldehyde for 2 h at 4˚C followed by 1% osmium tetroxide for 1 h at room temperature. The samples were dehydrated at room temperature using a series of acetone solutions of increasing concentration. Subsequently, they were counterstained in a saturated solution of uranyl acetate for 2 h at room temperature, followed by lead citrate treatment for 40 min at room temperature. Finally, sections (60 nm) were examined using a transmission electron microscope at a magnification of x50,000. In addition, the morphological changes in type II alveolar epithelial cells and macrophages from the lungs were also observed by electron microscopy. The morphological features of type II alveolar epithelial cells include large nuclei and multiple vacuoles, and mitochondria and rough endoplasmic reticulum in the cytoplasm (31). The surfaces of macrophages were covered with multiple irregular folds, microvilli and pseudopods; the cytoplasm contained a large number of lysosomes, phagosomes and vesicles; and there were many microfilaments and microtubules near the cell membrane (32).

Hematoxylin and eosin staining. All samples were treated with 4% paraformaldehyde (cat. no. #P6148, Sigma-Aldrich; Merk KGaA) for 24 h at 4˚C. The samples were then treated with hematoxylin (cat. no. ZLI-9609; OriGene Technologies, Inc., Rockville, MD, USA) for 10 min, 70% ethanol and 1% hydrochloric acid at 25˚C. The sections (4-μm-thick) were stained with 0.1% eosin (Surgipath®; Leica Microsystems, Ltd., Milton Keynes, UK) for 30 sec, and dehydrated in 80%, 90 and 100% ethanol at 25˚C. Ethanol was used to dehydrate the sections at 25˚C and the results were examined under an optical microscope (Eclipse E100; Nikon Corporation, Tokyo, Japan; magnification, x100).

ELISA. At the end of treatment in mice, blood was collected from mice and rapidly centrifuged at 5,000 x g for 10 min at 4˚C. The supernatants were stored at -20˚C until analysis. ELISA kits for mouse IL-4 (cat. no. EK0405; Boster Biological Technology, Pleasanton, CA, USA), TNF-α (CSB-E04741m) and TGF-β1 (CSB-E4726m; both Cusabio Technology LLC, Wuhan, China) were used according to the manufacturers' protocol.

Double immunofluorescence staining. Lung tissues collected from mice were fixed, cut into sections and stained using the standard procedure (33). The slides were examined and photographed using fluorescence microscopy (ECLIPSE TI-SR; Nikon Corporation) using a magnification of x100. The slides were blocked with 5% bovine serum albumin (cat. no. A7638; Sigma Aldrich; Merck KGaA, Darmstadt, Germany) for 1 h at room temperature. The slides were incubated with primary antibodies at 4˚C overnight. The following day, the slides were incubated with fluorescence-conjugated secondary antibodies (1:200; cat. no. A-11029; Alexa Fluoro, Molecular Probes; Thermo Fisher Scientific, Inc.) for 1 h at room temperature. The fluorescence intensities of CD68, F4/80, CD163 and HLA-DR were calculated using Image Pro Plus 6.0 software (Media Cybernetics, Inc., Rockville, MD, USA). The following primary antibodies were used: Anti-CD68 (1:25; cat. no. ab201844), anti-F4/80 (1:100; cat. no. ab100790), anti-CD163 (1:10; cat. no. ab17051) and anti-HLA-DR (1:500; cat. no. ab226820; all Abcam, Cambridge, UK).

Reverse transcription-quantitative polymerase chain reaction (RT-qPCR) analysis. The RNA was extracted from the lung tissues by using TRIzol reagent (cat. no. #9109; Takara Bio Inc., Otsu, Japan) and its concentration was measured using the Nanodrop 2000 Spectrophotometer (Thermo Fisher Scientific, Inc.). RNA was reverse transcribed into cDNA by using the Reverse Transcription kit (cat. no. RR037A; Takara Bio Inc.) according to the manufacturer's protocol. The qPCR was performed using the TB Green Premix Ex TaqII kit (cat. no RR820A; Takara Bio Inc.). The reaction system was performed in a volume of 20 μl and the thermocycling conditions were as follows: Initial denaturation at 95˚C for 30 sec, and 40 cycles of 95˚C for 5 sec and 60˚C for 34 sec.

Gene expression was normalized to the level of GAPDH within each sample using the $2^{-\Delta\Delta Cq}$ methods (34). Gene expression was shown as expression relative to the indicated controls. The specific primers were: IL-4: 5'-AACGAGGTCACAGGA GAAGG-3' (forward), 5'-TCTGCAGCTCCATGAGAACA-3' (reverse); TNF-α: 5'-AGGTCCAGCTCTTTTCCTCC-3' (forward), 5'-TGGGGCTGAAGTGTAGATGG-3' (reverse); TGF-β1: 5'-TCGCTTTGTACAACAGCACC-3' (forward), 5'-ACTGCTTCCCGAATGTCTGA-3' (reverse); and GAPDH: 5'-ATGGTGAAGGTCGGTGTGAA-3' (forward), 5'-TGG AAGATGGTGATGGGCTT-3' (reverse).

Western blotting. Protein extraction and blotting were performed as previously described (35). Proteins were extracted using RIPA buffer (Beyotime Institute of Biotechnology, Shanghai, China). Following the determination of protein concentration by a Protein Determination kit (cat. no. 704002; Cayman Chemical Company, Inc., Ann Arbor, MI, USA), equal amounts of protein samples (20 μg loaded per lane) were size-fractioned using SDS-PAGE (8% gels), electrotransferred onto a polyvinylidene difluoride membrane (Bio-Rad Laboratories, Inc., Hercules, CA, USA). The membranes were blocked with 5% skimmed milk (BD Biosciences), and then were hybridized with primary antibodies overnight at 4˚C. After washing, the membranes were incubated with horseradish peroxidase conjugated secondary antibodies (1:10,000; cat. no. #W4011; Promega Corporation, Madison, WI, USA) for 2 h at room temperature. Finally, the enhanced chemiluminescent reagents (MILLIPORE, WBKLS0500) was used to treat the membranes. Densitometric quantification of bands was performed using the ImageJ software (version 1.50; National Institutes of Health, Bethesda, MD, USA). The following primary antibodies were used: Anti-GAPDH (cat. no. ab9485; 1:2,500), anti-IL-4 (cat. no. ab9811), anti-TNF-α (cat. no. ab6671) and anti-TGF-β1 (cat. no. ab92486; all 1:1,000; all Abcam).

Statistical analysis. All data were analyzed using SPSS 19.0 software (IBM Corp., Armonk, NY, USA) with Student's t-test and reported as mean ± standard error of the mean (n=10). P<0.05 indicated that the difference between groups was statistically significant.

Results

NO_x and $PM_{2.5}$ concentrations are markedly high, and CO concentrations markedly fluctuate in the underground parking lot. The atmospheric pollutants, CO, NO_x and $PM_{2.5}$, were examined (Fig. 1). In the cage in the laboratory, the levels of CO, NO_x and $PM_{2.5}$ were stable at ~2, 0.01, and 0.08 mg/m³, respectively. In the cage in the underground garage, NO_x and $PM_{2.5}$ fluctuated considerably and were markedly higher compared with those levels in the laboratory at all time-points (7:00 am to 6:00 pm), whereas CO levels were increased in the underground garage compared with the laboratory at 12:00, 16:00 and 17:00 pm.

Atmospheric pollutants induce lung damage. The morphological changes in type II alveolar epithelial cells and macrophages from the lungs were examined by electron microscopy (Fig. 2A and B). In the control mice, microvilli and lamellar bodies were abundant in type II alveolar epithelial cells, which did not exhibit intracellular edema (Fig. 2A). In mice fed in the underground garage, the microvilli and the lamellar bodies were markedly reduced in type II alveolar epithelial cells. The size of lamellar bodies also decreased. In addition, intracellular edema was present in the type II alveolar epithelial cells. These findings indicated functional impairment of the cells.

In the control mice, macrophages contained a few low-density particles, but not the high-density particles of inorganic substances (Fig. 2B). The observed particles could have been bacteria or products of decomposition, such as remnants of cell necrosis. In the polluted group, there was a large number of high-density inorganic particles in the lung macrophages. The particles deposited in the lungs were $PM_{2.5}$ from diesel exhaust pollution, which may have activated the macrophages.

Thus, the changes in the morphology of type II alveolar epithelial cells and macrophages suggested that diesel exhaust induced lung damage. During the study, no changes in the
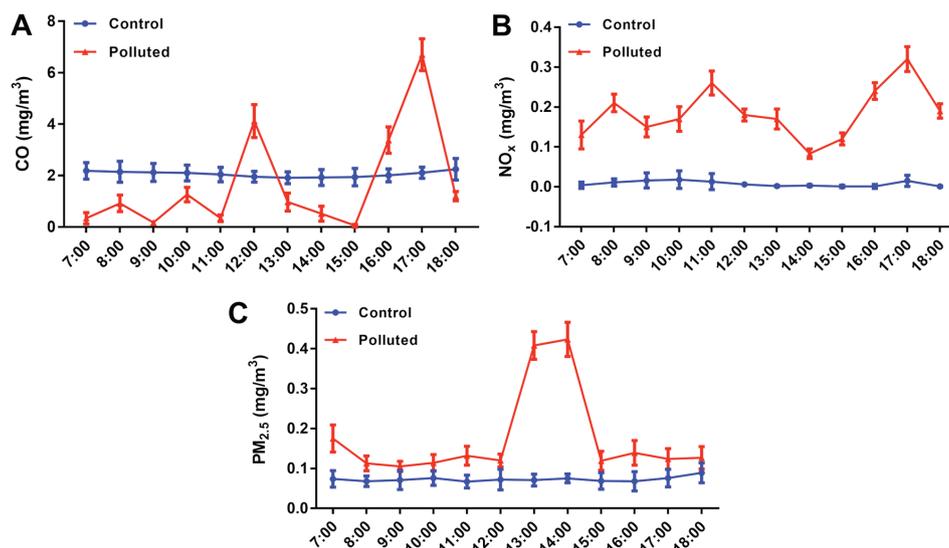
Figure 1. NO$_x$ and PM$_{2.5}$ concentrations are markedly high, and CO concentrations markedly fluctuate in the underground parking lot. The concentration of (A) CO, (B) NO$_x$ and (C) PM$_{2.5}$ were measured in an underground parking lot and a laboratory 12 times a day. PM$_{2.5}$, particulate matter with an aerodynamic diameter smaller than 2.5 µm.
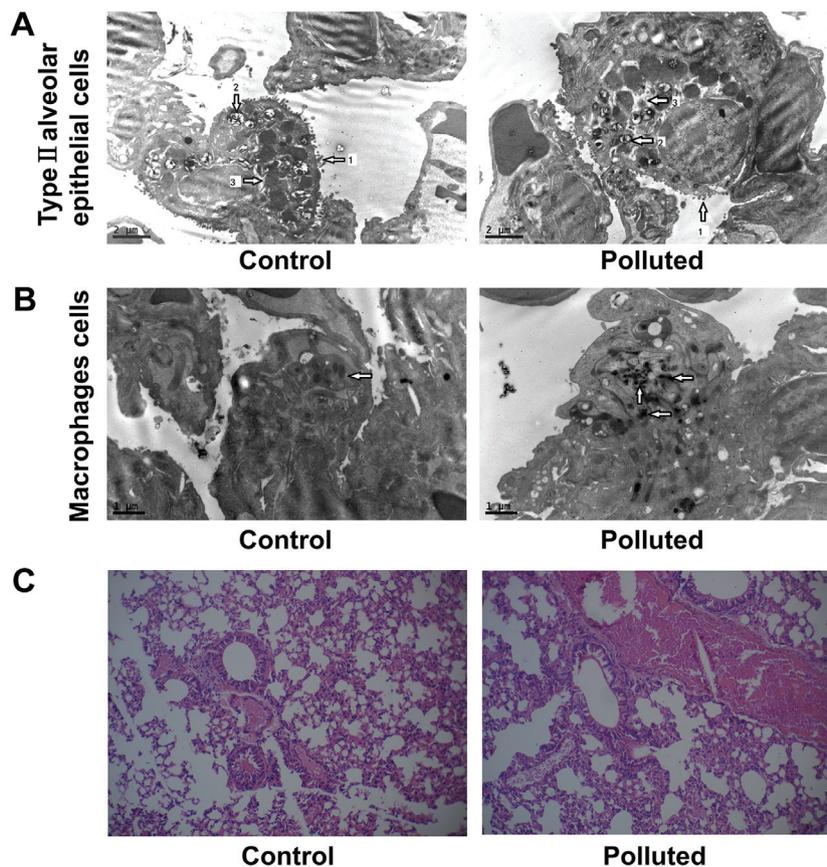

Figure 2. Atmospheric pollutants induce lung damage. (A) The ultrastructures of type II alveolar epithelial cells were observed by transmission electron microscope in the control and polluted group. Magnification, x5,800. The arrows indicate cell surface villi (1), lamellar body (2) and cytoplasm (3). (B) The ultrastructures of macrophages were observed by transmission electron microscope in the control and polluted group. Magnification, x9,700. Arrows indicate intracellular phagocytes. (C) The morphological structures were detected by haematoxylin and eosin staining in the control and polluted group. Magnification, x100.

body weight or clinical parameters of the mice were observed (data not shown).

Furthermore, morphological structures of lung tissue were assessed by H&E staining in the control and polluted groups (Fig. 2C). The tissues were comparatively complete and the nuclei were clearly visible in the control group, while the tissues were damaged in the polluted group. The number of inflammatory cells, including neutrophils, polylymphocytes
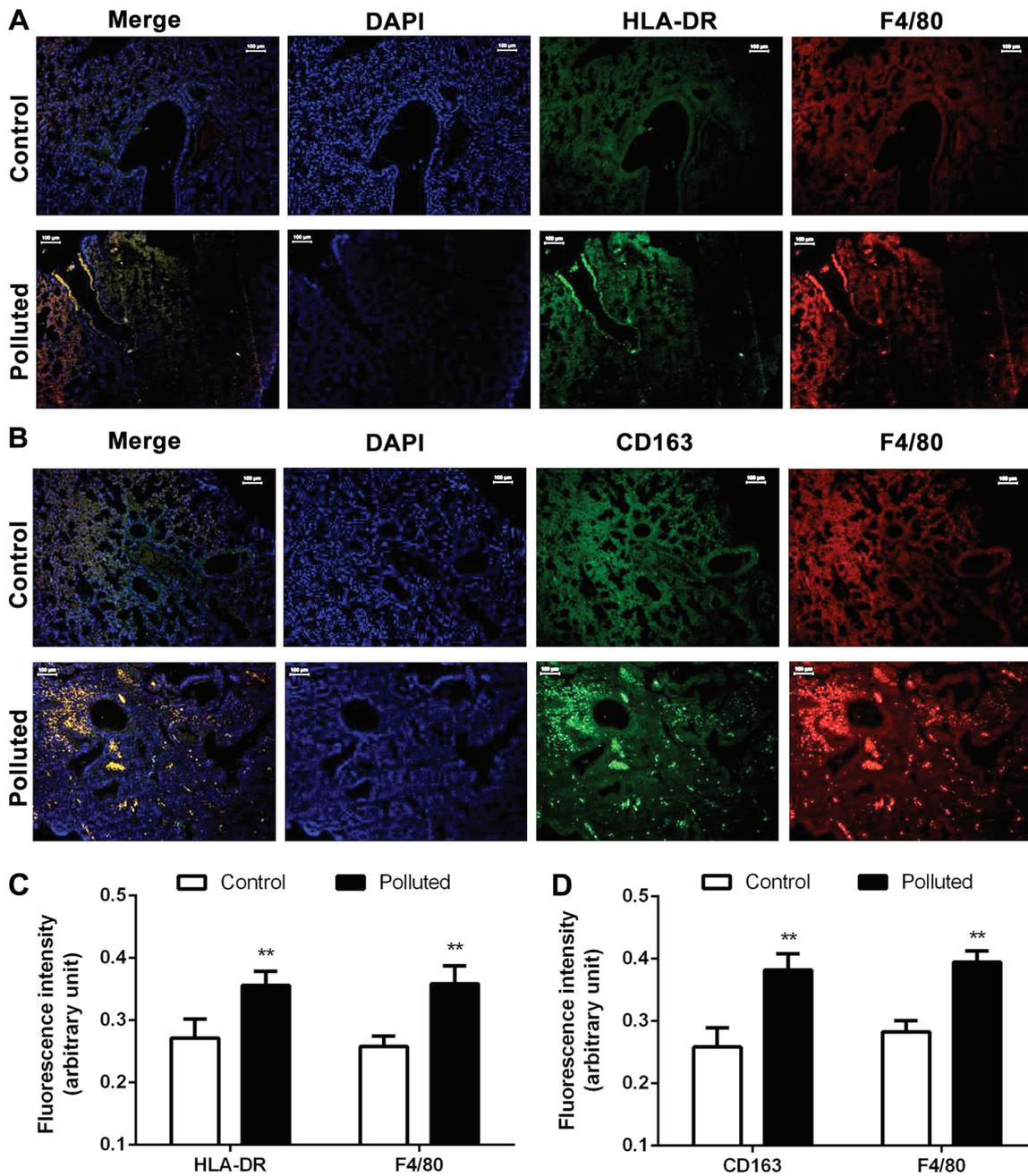
Figure 3. HLA-DR, CD163 and F4/80 protein expression increases in the lungs of the polluted group. Immunofluorescence of (A) HLA-DR (green) and F4/80 (red), and (B) CD163 (green) and F4/80 (red). Scale bar, 100 µm. Quantitative analysis of the immunofluorescence staining density of the paired (C) HLA-DR and F4/80, and (D) CD163 and F4/80 protein expression. **$P<0.01$ vs. Control. F4/80; adhesion G protein-coupled receptor E1; HLA, human leukocyte antigen; CD, cluster of differentiation.

and eosinophils, increased in the polluted group compared with the control group (data not shown).

HLA-DR, CD163 and F4/80 protein expression increases in the lungs of the polluted group. To further confirm the lung injury, double immunofluorescence staining for HLA-DR and F4/80, which are expressed in M1 polarized macrophages (36), and for CD163 and F4/80, which are expressed in M2 polarized macrophages, was performed (Fig. 3). In the polluted group, HLA-DR and F4/80 expression levels were markedly increased, while CD163 and F4/80 expression levels were also markedly increased (Fig. 3A and B).

The protein expression levels of HLA-DR and F4/80 were significantly increased in the polluted group compared with the control group, suggesting an increased number of M1 polarized macrophages, which express HLA-DR (Fig. 3C). Similarly, CD163 and F4/80 protein expression levels were significantly increased in the polluted group, suggesting an increased number of M2 polarized macrophages, which express CD163 (Fig. 3D). Thus, the numbers of M1 and M2 macrophages were increased, and M1 and M2 macrophages infiltrated the tissue. CD163 and HLA-DR could thus be used for monitoring the extent of lung injury in a polluted environment.
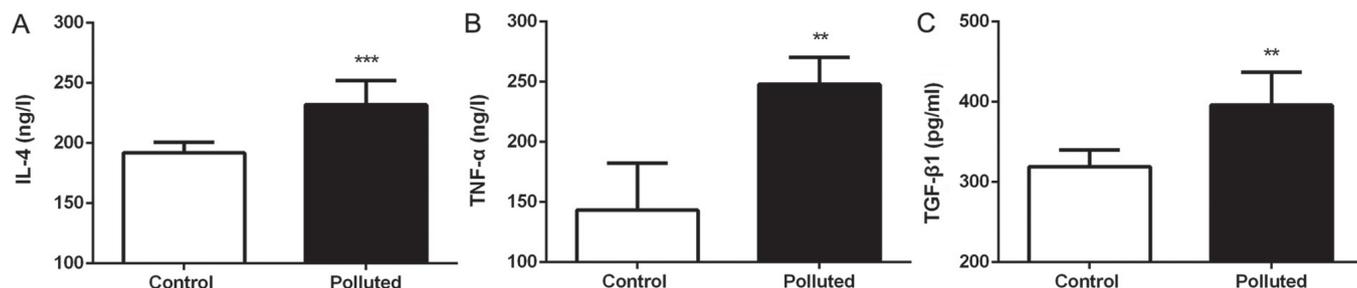
Figure 4. IL-4, TNF-α and TGF-β1 serum levels increase in the polluted group. The concentrations of serum (A) IL-4, (B) TNF-α and (C) TGF-β1 were measured using ELISA. **$P<0.01$, ***$P<0.001$ vs. Control. IL, interleukin; TNF, tumor necrosis factor; TGF, transforming growth factor.
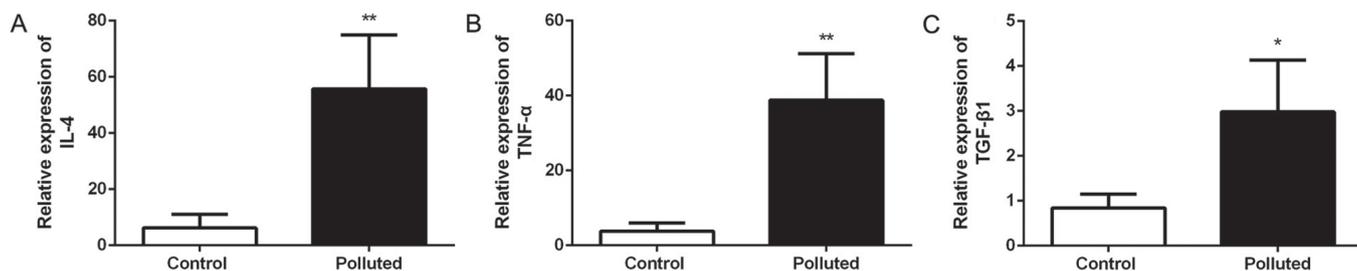

Figure 5. IL-4, TNF-α and TGF-β1 mRNA levels increase in the lungs of the polluted group. (A) IL-4, (B) TNF-α and (C) TGF-β1 mRNA levels were detected by using reverse transcription-quantitative polymerase chain reaction. *$P<0.05$, **$P<0.01$ vs. Control. IL, interleukin; TNF, tumor necrosis factor; TGF, transforming growth factor.

IL-4, TNF-α and TGF-β1 serum levels increase in the polluted group. The serum levels of the cytokines, IL-4, TNF-α and TGF-β1, were examined (Fig. 4). In the mice fed in the polluted environment, the serum levels of IL-4 (Fig. 4A), TNF-α (Fig. 4B) and TGF-β1 (Fig. 4C) were significantly increased compared with those mice fed in the laboratory.

IL-4, TNF-α and TGF-β1 mRNA and protein levels increase in the lungs of the polluted group. The mRNA and protein levels of the cytokines, IL-4, TNF-α, and TGF-β1, in lung tissues were assessed by RT-qPCR (Fig. 5) and western blotting (Fig. 6). Atmospheric pollutants significantly upregulated the mRNA levels of IL-4 (Fig. 5A), TNF-α (Fig. 5B) and TGF-β1 (Fig. 5C), as well as markedly (Fig. 6A) and significantly (Fig. 6A) upregulating the protein levels of IL-4, TNF-α and TGF-β1. Thus, atmospheric pollutants increased the levels of these cytokines in lung tissues.

Discussion

The authors of the current study demonstrated that the levels of three representative indicators of pollution, CO, NO$_x$ and PM$_{2.5}$, in an underground parking lot were significantly higher compared with those in the laboratory. The air quality in the laboratory met the requirements of GB3095-2012 standard class II of China, while, in the underground parking lot, the pollution levels exceeded the national standard by far (37).

Numerous acute toxicological experiments using single components of diesel exhaust confirmed that a variety of these components can lead to an increased production of oxygen free radicals, thus directly damaging lung cells and influencing digestive function, growth, and development by
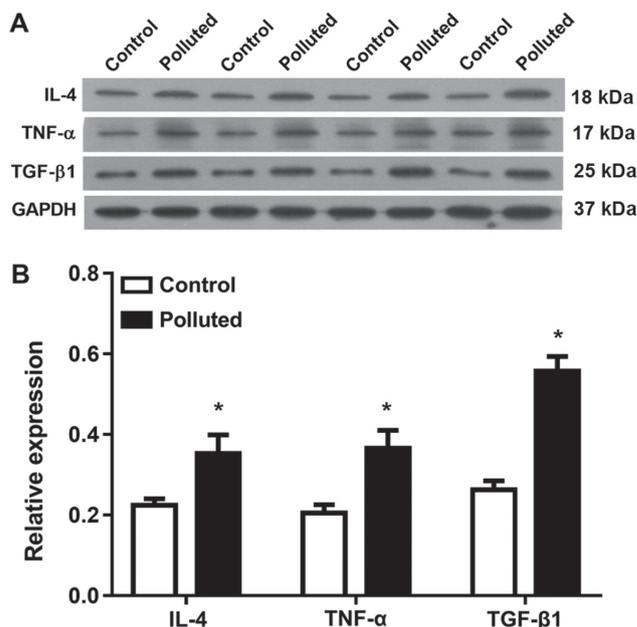

Figure 6. IL-4, TNF-α and TGF-β1 protein levels increase in the lungs of the polluted group. (A) Western blot analysis and (B) densitometric quantification of IL-4, TNF-α and TGF-β1 bands were performed in lung tissues. *$P<0.05$ vs. Control. IL, interleukin; TNF, tumor necrosis factor; TGF, transforming growth factor.

negatively affecting Ca^{2+} balance (11). After feeding in the polluted environment for 3 months, findings revealed that atmospheric pollutants could induce lung damage. In addition, it was determined that the number of inflammatory cells increased, including neutrophils, lymphocytes and eosinophils.

These results support the hypothesis that lung injury can be induced by oxygen free radicals. Previous research has shown that particulate matter exposure could change macrophage morphology (8,38), which is consistent with the observation of macrophages in lung tissue using electron microscopy. The deposition of a large number of dust particles in macrophages has been demonstrated to induce macrophage apoptosis, which is also mediated by an increase in oxygen free radicals and injury of mitochondria in macrophages (39-41). If the deposition becomes more serious, macrophages are overburdened, eventually leading to decreased phagocytosis, thus influencing immune defense function (42). The change in oxygen free radicals was not evaluated in the current study.

Research has demonstrated that M1-polarized macrophages expressing HLA-DR have a pro-inflammatory effect, while M2-polarized macrophages expressing CD163 have the function of immunosuppressive tissue repair (43). The present results indicated that the number of M1 and M2 macrophages increased, and there was a large number of macrophage aggregation and infiltration in lung tissues of mice that were fed in the polluted environment. Therefore, the increase of M1 and M2-polarized macrophages may be an important cause of immune dysfunction caused by pollution. Particles/dust are solid or liquid particulate matter in the atmosphere (44). According to particle size, particles can be divided into total suspended particles and inhalable particles. Inhalable particles can be divided into coarse particles (PM10: aerodynamic diameter between 2.5-10 μm) and fine particles (PM2.5 ≤2.5 μm) (45). As an important air pollutant, particle size, shape and composition are associated with health (46). Previous research showed that inhalable particles are responsible for chronic lung injury (47). A large number of studies have confirmed that, due to their very small size, PM_{10} particles easily enter the lungs (48,49). With adsorption of heavy metals and other toxic substances, the surface area of those particles becomes relatively large (50,51). As a result, PM_{10} induces a potent inflammatory effect by increasing intracellular Ca^{2+}, as well as the phenotypic transition of macrophages to M1 macrophages (52). The pollutants in the range from $PM_{2.5}$ to PM_{10} have been demonstrated to induce respiratory burst in RAW264.7 cells, promoting the formation of a large number of oxygen free radicals, the imbalance of the oxidant and antioxidant system, and epithelial cell damage with increased epithelium permeability, all eventually resulting in chronic lung injury (8-10). The lung injury in turn promotes the phenotypic transition of macrophages to M2 macrophages (53). The excessive increase in M2 macrophage numbers has been demonstrated to have negative consequences, including pulmonary immune suppression, and an increased incidence of pulmonary fibrosis and lung cancer (54,55).

The experimental results by ELISA demonstrated that the serum levels of IL-4, TNF-α and TGF-β1 in the polluted group were significantly higher compared with the control group. Similar results were observed in the lung tissues. The mRNA and protein levels of IL-4, TNF-α and TGF-β1 in the polluted group were also significantly higher compared with the control group. The increase in the level of proteins was evidently less compared with that of mRNAs, which may be due to the regulation of the expression at the translation level.

In vivo studies have revealed that the expression of TGF-β1 is positively correlated with the duration of exposure to and the amount of atmospheric particulate matter, such as $PM_{2.5}$, in the environment (13-17). It was also demonstrated that the serum levels of IL-4 and TNF-α were positively correlated with the duration of exposure to air pollution and that IL-4 levels were correlated with gaseous pollutants, such as NO_x, while TNF-α levels were correlated with particulate matter, such as $PM_{2.5}$ (18,19). Those results are consistent with our findings. The mechanism of increased levels of inflammatory cytokines in mice may be associated with the oxidative damage of the respiratory mucosa by gaseous pollutants, such as NO_x, the stimulation of the lung epithelial cells by $PM_{2.5}$ and transition metals present in $PM_{2.5}$ (56).

IL-4 is an important cytokine in the regulation of T lymphocytes and the synthesis of immunoglobulin (Ig) E by B lymphocytes (57). An increase in IL-4 promotes the secretion of IgE, which is key for the onset of allergic diseases (58). This is also consistent with epidemiological surveys that revealed that air pollution results in an increase in IgE levels and a higher incidence of chronic pulmonary diseases, including asthma and chronic obstructive pulmonary disease (59,60). TNF-α is an important inflammatory factor and immunoregulatory factor; its overexpression has been determined to promote the aggregation of a variety of inflammatory cells, leading to abnormal inflammatory response, immune dysfunction or a variety of inflammatory diseases (61). Many studies have revealed that TGF-β1 is a potent chemokine for fibroblasts (62-64). In lung tissues, TGF-β1 upregulates the expression of collagen and fibronectin to promote an increase of the extracellular matrix; meanwhile, it downregulates the secretion of proteases, but increases the secretion of protease inhibitors to inhibit the degradation of the extracellular matrix, thus participating in lung fibrosis (65). In a study of the morphological changes in the chronic lung injury of rats caused by gasoline exhaust pollution, inflammatory reactions were observed in the first 2 weeks, followed by lung fibroblast hyperplasia after 4 weeks. The hyperplasia of fibroblasts was increasingly evident with time and has been associated with chronic inflammatory reaction (21,22). Recent research has indicated that TNF-α and TGF-β1 promotes the development of inflammation and pulmonary fibrosis (66,67).

In conclusion, the sub-chronic exposure to a highly polluted environment, such as that with high $PM_{2.5}$ levels, can lead to lung injury in mice. Although ultrastructural damage, and local and systemic immune imbalance was observed, further studies should focus on the protection of lungs against injury caused by polluted environments.

Availability of data and materials

All data generated or analyzed during the present study are included in this published article.

Authors' contributions

JY, YC and ZM conceived and supervised the study; YC, ZY and HD designed and performed experiments; JY, YC and ZM analyzed data, wrote the manuscript and made manuscript revisions. All authors read and approved the final manuscript.

Ethics approval and consent to participate

The present study was approved by the Experimental Animal Ethics Committee Center of The First Affiliated Hospital of Sun Yat-sen University (Guangzhou, China; animal certificate no. 4408500931).

Patient consent for publication

Not applicable.

Competing interests

The authors declare that they have no competing interests.

References

1. Brown MJ, Williams MD, Nelson MA and Werley KA: QUIC transport and dispersion modeling of vehicle emissions in cities for better public health assessments. Environ Health Insights 9 (Suppl 1): S55-S65, 2016.
2. Guan WJ, Zheng XY, Chung KF and Zhong NS: Impact of air pollution on the burden of chronic respiratory diseases in China: Time for urgent action. Lancet 388: 1939-1951, 2016.
3. Pandey P, Patel DK, Khan AH, Barman SC, Murthy RC and Kisku GC: Temporal distribution of fine particulates (PM(2).(5):PM(1)(0)), potentially toxic metals, PAHs and Metal-bound carcinogenic risk in the population of Lucknow City, India. J Environ Sci Health A Tox Hazard Subst Environ Eng 48: 730-745, 2013.
4. Volk HE, Lurmann F, Penfold B, Hertz-Picciotto I and McConnell R: Traffic-related air pollution, particulate matter, and autism. JAMA Psychiatry 70: 71-77, 2013.
5. Zielinska B, Sagebiel J, McDonald JD, Whitney K and Lawson DR: Emission rates and comparative chemical composition from selected in-use diesel and gasoline-fueled vehicles. J Air Waste Manag Assoc 54: 1138-1150, 2004.
6. Ezzati M, Lopez AD, Rodgers A, Vander Hoorn S and Murray CJ; Comparative Risk Assessment Collaborating Group: Selected major risk factors and global and regional burden of disease. Lancet 360: 1347-1360, 2002.
7. IARC monographs on the evaluation of carcinogenic risks to humans. Diesel and gasoline engine exhausts and some nitroarenes. International Agency for Research on Cancer. IARC Monogr Eval Carcinog Risks Hum 46: 1-458, 1989.
8. Su R, Jin X, Zhang W, Li Z, Liu X and Ren J: Particulate matter exposure induces the autophagy of macrophages via oxidative stress-mediated PI3K/AKT/mTOR pathway. Chemosphere 167: 444-453, 2017.
9. Mitkus RJ, Powell JL, Zeisler R and Squibb KS: Comparative physicochemical and biological characterization of NIST interim reference material PM2.5 and SRM 1648 in human A549 and mouse RAW264.7 cells. Toxicol In Vitro 27: 2289-2298, 2013.
10. Liu XC, Li YJ, Wang YJ, Li Q, Yang Q, Weng XG, Chen Ying, Cai WY, Guo Y, Kan XX, *et al*: Protection of Shenlian extracts to PM2.5 infected RAW 264.7 cell damage. Zhongguo Zhong Yao Za Zhi 40: 1977-1983, 2015 (In Chinese).
11. Yanamala N, Hatfield MK, Farcas MT, Schwegler-Berry D, Hummer JA, Shurin MR, Birch ME, Gutkin DW, Kisin E, Kagan VE, *et al*: Biodiesel versus diesel exposure: Enhanced pulmonary inflammation, oxidative stress, and differential morphological changes in the mouse lung. Toxicol Appl Pharmacol 272: 373-383, 2013.
12. Zhou H and Fan X: Changes of Ca~(2+)-ATPase activity and oxygen free radicals in microsome membranes of postharvest peach fruit. Acta Botanica Boreali-Occidentalia Sinica 27: 1161-1166, 2007.
13. Libalova H, Uhlířová K, Kléma J, Machala M, Šrám RJ, Ciganek M and Topinka J: Global gene expression changes in human embryonic lung fibroblasts induced by organic extracts from respirable air particles. Part Fibre Toxicol 9: 1, 2012.
14. Dagher Z, Garçon G, Gosset P, Ledoux F, Surpateanu G, Courcot D, Aboukais A, Puskaric E and Shirali P: Pro-inflammatory effects of Dunkerque city air pollution particulate matter 2.5 in human epithelial lung cells (L132) in culture. J Appl Toxicol 25: 166-175, 2005.
15. Xie Y, Zhang X, Tian Z, Jiang R, Chen R, Song W and Zhao J: Preexposure to PM2.5 exacerbates acute viral myocarditis associated with Th17 cell. Int J Cardiol 168: 3837-3845, 2013.
16. Furuyama A, Hirano S, Koike E and Kobayashi T: Induction of oxidative stress and inhibition of plasminogen activator inhibitor-1 production in endothelial cells following exposure to organic extracts of diesel exhaust particles and urban fine particles. Arch Toxicol 80: 154-162, 2006.
17. Furuyama A and Mochitate K: Hepatocyte growth factor inhibits the formation of the basement membrane of alveolar epithelial cells in vitro. Am J Physiol Lung Cell Mol Physiol 286: L939-L946, 2004.
18. Nerriere E, Zmirou-Navier D, Blanchard O, Momas I, Ladner J, Le Moullec Y, Personnaz MB, Lameloise P, Delmas V, Target A and Desqueyroux H: Can we use fixed ambient air monitors to estimate population long-term exposure to air pollutants? The case of spatial variability in the Genotox ER study. Environ Res 97: 32-42, 2005.
19. Hystad P, Demers PA, Johnson KC, Carpiano RM and Brauer M: Long-term residential exposure to air pollution and lung cancer risk. Epidemiology 24: 762-772, 2013.
20. Wang Y, *et al*: Study on the morphological changes of the rats' lung caused by exhausting of gasoline engine. Xian Dai Yu Fang Yi Xue 39: 1349-1354, 2012 (In Chinese).
21. Ali BH, Al Za'abi M, Shalaby A, Manoj P, Waly MI, Yasin J, Fahim M and Nemmar A: The effect of thymoquinone treatment on the combined renal and pulmonary toxicity of cisplatin and diesel exhaust particles. Exp Biol Med (Maywood) 240: 1698-1707, 2015.
22. Akopian AN, Fanick ER and Brooks EG: TRP channels and traffic-related environmental pollution-induced pulmonary disease. Semin Immunopathol 38: 331-338, 2016.
23. Yang J, Chen Y, Yu Z, Ding H and Ma Z: Changes in gene expression in lungs of mice exposed to traffic-related air pollution. Mol Cell Probes 39: 33-40, 2018.
24. Li C, Shi M, Li S, Bai Z and Wang Z: Combined use of land use regression and BenMAP for estimating public health benefits of reducing PM 2.5 in Tianjin, China. Atmospheric Environ 152: 16-23, 2017.
25. Chen Y, *et al*: A study on effect of automobile exhaust pollutants in underground parking area on serum inflammatory cytokines of mice. Zhongguo Zhong Xi Yi Ji Jiu Za Zhi 2013: 353-356, 2013 (In Chinese).
26. Wang G, Zhen L, Lü P, Jiang R and Song W: Effects of ozone and fine particulate matter (PM2.5) on rat cardiac autonomic nervous system and systemic inflammation. Wei Sheng Yan Jiu 42: 554-560, 2013 (In Chinese).
27. Pei Y, Jiang R, Zou Y, Wang Y, Zhang S, Wang G, Zhao J and Song W: Effects of fine particulate matter (PM2.5) on systemic oxidative stress and cardiac function in ApoE(-/-) mice. Int J Environ Res Public Health 13: E484, 2016.
28. Wang H, An J, Cheng M, Shen L, Zhu B, Li Y, Wang Y, Duan Q, Sullivan A and Xia L: One year online measurements of water-soluble ions at the industrially polluted town of Nanjing, China: Sources, seasonal and diurnal variations. Chemosphere 148: 526-536, 2016.
29. Zhao G, Li S, Hong G, Li M, Wu B, Qiu Q and Lu Z: The effect of resveratrol on paraquat-induced acute lung injury in mice and its mechanism. Zhonghua Wei Zhong Bing Ji Jiu Yi Xue 28: 33-37, 2016 (In Chinese).
30. Sun CZ, Shen H, He XW, Bao L, Song Y, Zhang Z and Qin HD: Effect of dobutamine on lung aquaporin 5 in endotoxin shock-induced acute lung injury rabbit. J Thorac Dis 7: 1467-1477, 2015.
31. Ten Have-Opbroek AA, Otto-Verberne CJ and Dubbeldam JA: Ultrastructural characteristics of inclusion bodies of type II cells in late embryonic mouse lung. Anat Embryol (Berl) 181: 317-323, 1990.
32. Dale D: Neutropenia and neutrophilia. In: Lichtman M, Beutler E and Kipps TJ (eds): Williams Hematology. Seventh Edition. McGraw-Hill Professional, New York, NY, pp701-708, 2006.

33. Bronkhorst IH, Ly LV, Jordanova ES, Vrolijk J, Versluis M, Luyten GP and Jager MJ: Detection of M2-macrophages in uveal melanoma and relation with survival. Invest Ophthalmol Vis Sci 52: 643-650, 2011.
34. Livak KJ and Schmittgen TD: Analysis of relative gene expression data using real-time quantitative PCR and the 2(-Delta Delta C(T)) method. Methods 25: 402-408, 2001.
35. Zeng Y, Yao X, Chen L, Yan Z, Liu J, Zhang Y, Feng T, Wu J and Liu X: Sphingosine-1-phosphate induced epithelial-mesenchymal transition of hepatocellular carcinoma via an MMP-7/syndecan-1/TGF-β autocrine loop. Oncotarget 7: 63324-63337, 2016.
36. Schiechl G, Bauer B, Fuss I, Lang SA, Moser C, Ruemmele P, Rose-John S, Neurath MF, Geissler EK, Schlitt HJ, et al: Tumor development in murine ulcerative colitis depends on MyD88 signaling of colonic F4/80+CD11bhighGr1low macrophages. J Clin Invest 121: 1692-1708, 2011.
37. Chen L, Shi M, Gao S, Li S, Mao J, Zhang H, Sun Y, Bai Z and Wang Z: Assessment of population exposure to $PM_{2.5}$ for mortality in China and its public health benefit based on BenMAP. Environ Pollut 221: 311-317, 2017.
38. Long JF, Waldman WJ, Kristovich R, Williams M, Knight D and Dutta PK: Comparison of ultrastructural cytotoxic effects of carbon and carbon/iron particulates on human monocyte-derived macrophages. Environ Health Perspect 113: 170-174, 2005.
39. Huang YC, Soukup J, Harder S and Becker S: Mitochondrial oxidant production by a pollutant dust and NO-mediated apoptosis in human alveolar macrophage. Ajp Cell Physiol 284: C24-C32, 2003.
40. Lee KI, Whang J, Choi HG, Son YJ, Jeon HS, Back YW, Park HS, Paik S, Park JK, Choi CH and Kim HJ: Mycobacterium avium MAV2054 protein induces macrophage apoptosis by targeting mitochondria and reduces intracellular bacterial growth. Sci Rep 6: 37804, 2016.
41. Suen YK, Fung KP, Lee CY and Kong SK: Gliotoxin induces apoptosis in cultured macrophages via production of reactive oxygen species and cytochrome c release without mitochondrial depolarization. Free Radic Res 35: 1-10, 2001.
42. Zhang X, Zhong W, Meng Q, Lin Q, Fang C, Huang X, Li C, Huang Y and Tan J: Ambient PM2.5 exposure exacerbates severity of allergic asthma in previously sensitized mice. J Asthma 52: 785-794, 2015.
43. He H, Buckley M, Britton B, Mu Y, Warner K, Kumar S and Cory TJ: Polarized macrophage subsets differentially express the drug efflux transporters MRP1 and BCRP, resulting in altered HIV production. Antivir Chem Chemother 26: 204020661774516, 2018.
44. Liu D, Whitehead J, Alfarra MR, Villegas ER, Spracklen DV, Reddington CL, Kong S, Williams P, Haslett S, Taylor JW, et al: Black-carbon absorption enhancement in the atmosphere determined by particle mixing state. Nat Geosci 10: 184-188, 2017.
45. Huang H, Gao L, Xia D, Qiao L, Wang R, Su G, Liu W, Liu G and Zheng M: Characterization of short- and medium-chain chlorinated paraffins in outdoor/indoor PM10/PM2.5/PM1.0 in Beijing, China. Environ Pollut 225: 674-680, 2017.
46. Sui BL, Chen X, YU Y, Costa M and Wu H: Effect of particle size on particulate matter emissions during biosolid char combustion under air and oxyfuel conditions. 232: 251-256, 2018.
47. Gu LZ, Sun H and Chen JH: Histone deacetylases 3 deletion restrains PM2.5-induced mice lung injury by regulating NF-κB and TGF-β/Smad2/3 signaling pathways. Biomed Pharmacother 85: 756-762, 2017.
48. Pirela S, Molina R, Watson C, Cohen JM, Bello D, Demokritou P and Brain J: Effects of copy center particles on the lungs: A toxicological characterization using a Balb/c mouse model. Inhal Toxicol 25: 498-508, 2013.
49. Smith KR, Kim S, Recendez JJ, Teague SV, Ménache MG, Grubbs DE, Sioutas C and Pinkerton KE: Airborne particles of the california central valley alter the lungs of healthy adult rats. Environ Health Perspect 111: 902-908, 2003.
50. Mohammed MOA, Song WW, Ma YL, Liu LY, Ma WL, Li WL, Li YF, Wang FY, Qi MY, Lv N, et al: Distribution patterns, infiltration and health risk assessment of PM2.5-bound PAHs in indoor and outdoor air in cold zone. Chemosphere 155: 70-85, 2016.
51. Li M and Li YM: Fine particulate matter and nonalcoholic fatty liver disease. Zhonghua Gan Zang Bing Za Zhi 24: 713-715, 2016 (In Chinese).
52. Lee CC and Kang JJ: Extract of motorcycle exhaust particles induced macrophages apoptosis by calcium-dependent manner. Chem Res Toxicol 15: 1534-1542, 2002.
53. Akbarshahi H, Menzel M, Posaric Bauden M, Rosendahl A and Andersson R: Enrichment of murine CD68+ CCR2+ and CD68+ CD206+ lung macrophages in acute pancreatitis-associated acute lung injury. PLoS One 7: e42654, 2012.
54. Sun L, Chen B, Jiang R, Li J and Wang B: Resveratrol inhibits lung cancer growth by suppressing M2-like polarization of tumor associated macrophages. Cell Immunol 331: 86-93, 2017.
55. Kimura Y and Sumiyoshi M: Resveratrol prevents tumor growth and metastasis by inhibiting lymphangiogenesis and M2 macrophage activation and differentiation in tumor-associated macrophages. Nutr Cancer 68: 667-678, 2016.
56. Clarke RW, Catalano PJ, Koutrakis P, Murthy GG, Sioutas C, Paulauskis J, Coull B, Ferguson S and Godleski JJ: Urban air particulate inhalation alters pulmonary function and induces pulmonary inflammation in a rodent model of chronic bronchitis. Inhal Toxicol 11: 637-656, 1999.
57. Aversa G, Punnonen J and de Vries JE: The 26-kD transmembrane form of tumor necrosis factor alpha on activated CD4+ T cell clones provides a costimulatory signal for human B cell activation. J Exp Med 177: 1575-1585, 1993.
58. Huang CZ, Yang J, Qiao HL and Jia LJ: Polymorphisms and haplotype analysis of IL-4Rα Q576R and I75V in patients with penicillin allergy. Eur J Clin Pharmacol 65: 895-902, 2009.
59. Nygaard UC, Samuelsen M, Aase A and Løvik M: The capacity of particles to increase allergic sensitization is predicted by particle number and surface area, not by particle mass. Toxicol Sci 82: 515-524, 2004.
60. Samuelsen M, Nygaard UC and Lovik M: Allergy adjuvant effect of particles from wood smoke and road traffic. Toxicology 246: 124-131, 2008.
61. Lin ZM, Ma M, Li H, Qi Q, Liu YT, Yan YX, Shen YF, Yang XQ, Zhu FH, He SJ, et al: Topical administration of reversible SAHH inhibitor ameliorates imiquimod-induced psoriasis-like skin lesions in mice via suppression of TNF-α/IFN-γ-induced inflammatory response in keratinocytes and T cell-derived IL-17. Pharmacol Res 129: 443-452, 2018.
62. Huang M, Su S, Yang L, Zhu L, Liu Z and Duan R: Effect of exogenous TGF-β1 on the cadmium-induced nephrotoxicity by inhibiting apoptosis of proximal tubular cells through PI3K-AKT-mTOR signaling pathway. Chem Biol Interact 269: 25-32, 2017.
63. Labour MN, Riffault M, Christensen ST and Hoey DA: TGFβ1-induced recruitment of human bone mesenchymal stem cells is mediated by the primary cilium in a SMAD3-dependent manner. Sci Rep 6: 35542, 2016.
64. Zhou X, Hu H, Balzar S, Trudeau JB and Wenzel SE: MAPK regulation of IL-4/IL-13 receptors contributes to the synergistic increase in CCL11/eotaxin-1 in response to TGF-β1 and IL-13 in human airway fibroblasts. J Immunol 188: 6046-6054, 2012.
65. Ghavami S, Yeganeh B, Zeki AA, Shojaei S, Kenyon NJ, Ott S, Samali A, Patterson J, Alizadeh J, Moghadam AR, et al: Autophagy and the unfolded protein response promote profibrotic effects of TGF-β1 in human lung fibroblasts. Am J Physiol Lung Cell Mol Physiol 314: L493-L504, 2018.
66. Puerta-Arias JD, Pino-Tamayo PA, Arango JC and González Á: Depletion of neutrophils promotes the resolution of pulmonary inflammation and fibrosis in mice infected with paracoccidioides brasiliensis. PLoS One 11: e0163985, 2016.
67. Zaafan MA, Zaki HF, El-Brairy AI and Kenawy SA: Pyrrolidinedithiocarbamate attenuates bleomycin-induced pulmonary fibrosis in rats: Modulation of oxidative stress, fibrosis, and inflammatory parameters. Exp Lung Res 42: 408-416, 2016.